Article:
Palacios, A and Bradley, D (2021) Conversion of natural gas jet flame burners to hydrogen. International Journal of Hydrogen Energy, 46 (33). pp. 17051-17059. ISSN 0360-3199

https://doi.org/10.1016/j.ijhydene.2021.02.144

Conversion of Natural Gas Jet Flame Burners to Hydrogen

Adriana Palacios[1,*] and Derek Bradley[2]

[1]*Universidad de las Americas, Puebla, Department of Chemical, Food and Environmental Engineering, Puebla, Mexico.*

[2]*University of Leeds, School of Mechanical Engineering, Leeds, UK.*

**Corresponding author:* adriana.palacios@udlap.mx

Abstract

In a study of conversion from CH_4 to H_2, jet flame characteristics of these gases and their blends are compared on a burner diameter scale of mm. Low velocity H_2 and CH_4 jets, burned on pipes of different diameters, indicate higher blow-off limits for H_2, but lower heat release rates, a consequence of its lower specific energy. Compensation for this might be obtained through increased H_2 flow velocity, or a small increase in pipe diameter. Blended CH_4/H_2 flames have lower heat release rates than CH_4 alone, yet small proportions of H_2, with CH_4 might still be burned, on a CH_4 burner. Throughout, fundamental understanding is enhanced through two dimensionless groups: laminar flame thickness normalised by burner diameter, δ_k/D, and the dimensionless flow number, U^*. These suggest an optimal role for H_2 combustion, utilizing its high acoustic and blow-off velocities, in high intensity, subsonic, combustors, at low δ_k/D, and high U^*.

Keywords: conversion; hob-burners; blow-off; lifted flames; thermal power; burner flames.

Nomenclature

a_j	acoustic velocity at pipe exit plane (m/s)
C_p	specific heat at constant pressure (J/kg·K), at T^o
D	pipe diameter (m)
D_b	critical pipe diameter, below which blow-off can occur (m)
H_f	concentration of H_2 moles, as a fraction of the sum of those of H_2 and CH_4

k	thermal conductivity (W/m·K) at T^o
M_c	mass fraction of CH_4 in fuel, Eq. (4)
M_h	mass fraction of H_2 in fuel, Eq. (4)
M	Mach number at pipe exit plane, (u_j/a_j)
P_a	atmospheric pressure (Pa)
P_i	initial stagnation pressure (Pa)
Q	jet flame heat release rate, Eq. (4)
S_L	maximum laminar burning velocity of the fuel-air mixture at ambient atmosphere (m/s)
T^o	temperature at inner layer of laminar flame (K)
u_j	fuel flow velocity at exit plane of supply pipe (m/s)
U^*	dimensionless flow number for choked and un-choked flow, $(u_j/S_l)(\delta_k/D)^{0.4}(P_i/P_a)$
U_b^*	U^* value at blow-off

Greek

δ_k	$(k/C_p)_{T^o}/\rho_u S_L$ (m), Eqs. (1) and (2)
ΔH_c	heat of reaction of CH_4 (MJ/kg)
ΔH_h	heat of reaction of H_2 (MJ/kg)
ϕ	equivalence ratio
γ	ratio of specific heats
ρ	density (kg/m^3)
ρ_j	fuel density at atmospheric exit plane of pipe (kg/m^3)

Subscripts

a	ambient conditions
b	blow-off conditions
i	initial stagnation conditions
j	exit plane of pipe conditions

u unburned gas

1. Introduction

Studies of the conversion from methane to hydrogen initially have tended to concentrate on engine applications. The associated changes in combustion characteristics have been subjected to thorough analyses [1,2], as have the changes in turbulent burning velocities [3] and the chemical kinetics of laminar burning. Rather less effort has been devoted to the hydrogenation of the smaller boilers [4].

One approach to reducing the use of carbon fuels for heating has been progressively to replace natural gas with hydrogen. Gas burners often comprise an array of small diameter jet flames. However, jet flames of H_2 and of CH_4 have very different characteristics, in terms of their burning velocities, heat release rates, flame blow-off velocities, acoustic velocities, air requirements, flame lift-off distances, and propensities to flame quenching. The present study compares the burning characteristics of predominantly small jet flames of H_2, CH_4, and H_2/CH_4 mixtures. The paper does not deal with fuel/air premixed flames. With increasing fuel flow rates in lifted jet flames, eventually a point is reached at which the entrained air becomes excessive, reaction cannot be sustained, the flame extinguishes, and blows-off the burner. Prior to the onset of blow-off, computer studies [5-7] have shown the leading reaction zone flamelets to be of an equivalence ratio, ϕ, at which the laminar burning velocity attains its maximum value, S_L. On the basis of both mathematical modelling, and correlations of vast experimental data, extending over many fuels [5-8], the boundaries at which blow-off occurs have been expressed in terms of three dimensionless groups, a dimensionless flow number, U^*, involving the velocity ratio, u_j/S_L, pipe diameter, D/δ_k, and pressure ratio, P_i/P_a, with:

$$U^* = (u_j/S_L)(\delta_k/D)^{0.4}(P_i/P_a). \tag{1}$$

This includes the fuel flow velocity at the pipe exit plane, u_j, normalised by S_L, the pipe diameter normalised by the laminar flame thickness, D/δ_k, and (P_i/P_a), the ratio of initial stagnation to atmospheric pressure. Blow-off occurs in the final stage after an increase in flame lift-off distance. At blow-off, U^* is indicated by U_b^*, and D by D_b.

The chemically inert laminar flame preheat zone thickness, δ_k, that is employed is evaluated from the expression of Göttgens et al. [9]:

$$\delta_k = \frac{\left(k/C_p\right)_{To}}{\rho_u S_L}. \tag{2}$$

It defines the thickness of an inner layer, which is controlled by the location of a temperature T^o, below which there is no reaction. Calculated values of T^o for different gases are presented in [10]. The ratio of thermal conductivity to mass-based specific heat, $\left(k/C_p\right)_{To}$, is evaluated at the given values of T^o. Values of equivalence ratio, ϕ, at which S_L, is evaluated are noted, for 0.1 MPa and 300K. Hydrogen flames are unique, in that H atoms, created in the flame reaction zone, diffuse far upstream, where they can recombine. Consequently, in this case, the preheat zone is not completely chemically inert.

Boundaries of jet flame combustion regimes, particularly those involving lifted flames up to their blow-off limits, are usefully generalised by plots of D_b/δ_k, against U_b^*. Such plots are particularly useful for delineating different combustion regimes and, in the present context, those for CH_4, H_2 and their blends. The last are characterised by a parameter, H_f, equal to the ratio of H_2 moles to the total, $(CH_4 + H_2)$. Values of H_f for blends at blow-off were taken from the measurements of Wu et al. [10]. Necessary values of the maximum laminar burning velocity, S_L, in Eq. (1) for U^* were found for all values of H_f, and necessary values of ϕ from the measurements of premixed laminar burning velocities, of blends of Erjiang Hu et al. [11].

In summary, the present study first presents heat release rates, for different fuel jet velocities up to blow-off, and different burner pipe diameters of a few mm. The different combustion regimes are identified, interpreted, and meaningfully compared in plots of D_b/δ_k, against U_b^*.

Although, for different burner jet velocities, CH_4 has the highest heat release rates, H_2 has the highest blow-off velocities. Also, because of its higher acoustic velocity, H_2 has lowered Mach numbers and can sustain higher subsonic velocities. This makes high heat release rate hydrogen burners a possibility. Performances of the blended fuels are also scrutinised. Practically, these are of lower energy. Their only merit appears to be that, at low H_f, the combustion characteristics are similar to those of CH_4.

2. Derivation of Blow-off Characteristics of CH_4/H_2 Mixtures

Figure 1 shows, amongst other data, plots of of δ_k/D, against U_b* for both H_2 and CH_4, from [12]. The black circle symbols show the blow-off points for the CH_4/H_2 blends from [10, 11]. The blow-off measurements, taken from [10] involved blow-off of H_2/air flames, with increasing proportions of CH_4, using a 2 mm diameter burner. The necessary values of S_L, at the appropriate values of H_f and ϕ for these maximum values, were obtained from the measurements of premixed laminar burning velocities in [12]. These extended over full ranges of ϕ, at different H_f. Interestingly, the points on the present limiting blow-off curve for the changing H_2/CH_4 mixture are closer to the curve for pure H_2 than to that for pure CH_4.

Parts of the figure are taken from [12], and it also shows blow-off boundaries for several other Lifted Flames. Four major regimes are indicated, involving Laminar Flame Quench, Flame Blow-Off, Choked Flow, and Lifted Flames.

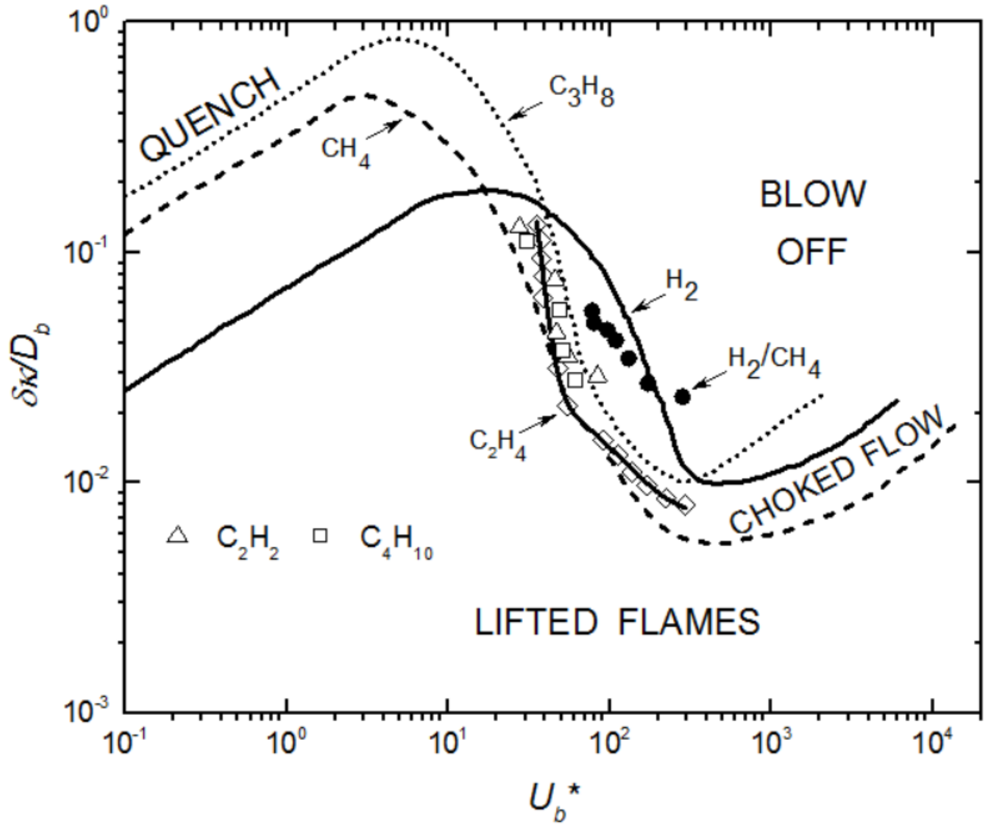

Fig. 1. Jet flame regimes. The black circle symbols show blow-off points for CH_4/H_2 blends from [10, 11]. Upper four black circle H_2/CH_4, symbols have H_f = 0.3, lower three H_f = 0.5. Other blow-off data, including those for CH_4 and H_2 are from mixtures in [12].

3. Hydrogen and Methane Fuel Jet Velocities and Heat Release Rates

It is necessary to characterise the fuel jet, in terms of the properties in Fig. 1, after a single expansion from the reservoir, within the supply pipe. This is from a stagnation pressure, P_i to atmospheric pressure, P_a, just outside the exit plane. This is followed by air entrainment by the jet. The flow is never supersonic. Values of S_L, necessary in the correlations, are listed in [12] for the different values of H_f and ϕ. As the flow expands, its Mach number, M, increases, according to the relationship [13,14]:

$$M^2 = 2/(\gamma - 1)[(P_i/P_a)^{(\gamma - 1)/\gamma} - 1], \quad (3)$$

with γ, the ratio of specific heats. As P_i/P_a and the jet velocity increase, the acoustic velocity at the leaving plane decreases with fuel temperature.

The product $M \cdot a_j$, yields the fuel velocity u_j. Values of a_j, along with other isentropic expansion data, and physico-chemical properties, are determined from the GasEq Code [15]. Values of U^* also are derived, in the process of evaluating u_j and δ_k. Fuel jet burners are characterised by their fuel mass flow rates, jet velocities, and heat release rates. When P_a/P_i becomes less than the Critical Pressure Ratio, the flow becomes choked, with the generation of shock waves in a complex flow beyond the exit plane [16]. Such flow is not a part of the present study, which features only subsonic values.

With a blend of the two fuels, the mass specific, energy density is $\rho_j\ (M_c \Delta H_c + M_h \Delta H_h)$, in which ρ_j is the fuel blend density at the exit plane, M_c and M_h, the respective mass fractions of CH_4 and H_2 in the combined blend. ΔH_c and ΔH_h are the respective, mass-based, heats of reaction, of CH_4 and H_2 in the combined blend. The overall heat release rate, Q, in the jet flame, is expressed by the product of the mass specific energy density, and the associated convective term. This is comprised of the product of the flow velocity, u_j, and pipe cross section area:

$$Q = u_j(\pi D^2/4)\rho_j(M_c \Delta H_c + M_h \Delta H_h). \tag{4}$$

No allowance is made for radiative heat loss, which only becomes significant at low u_j [17]. Fuel mass fractions are derived by multiplying mole concentrations in the mole fraction expressions, H_f, by their respective molecular weights, of 16.04 kg/kg mole for CH_4, and 2.015 kg/kg mole for H_2. Heats of reaction of ΔH_c, and ΔH_h, are 50 and 120 MJ/kg, respectively.

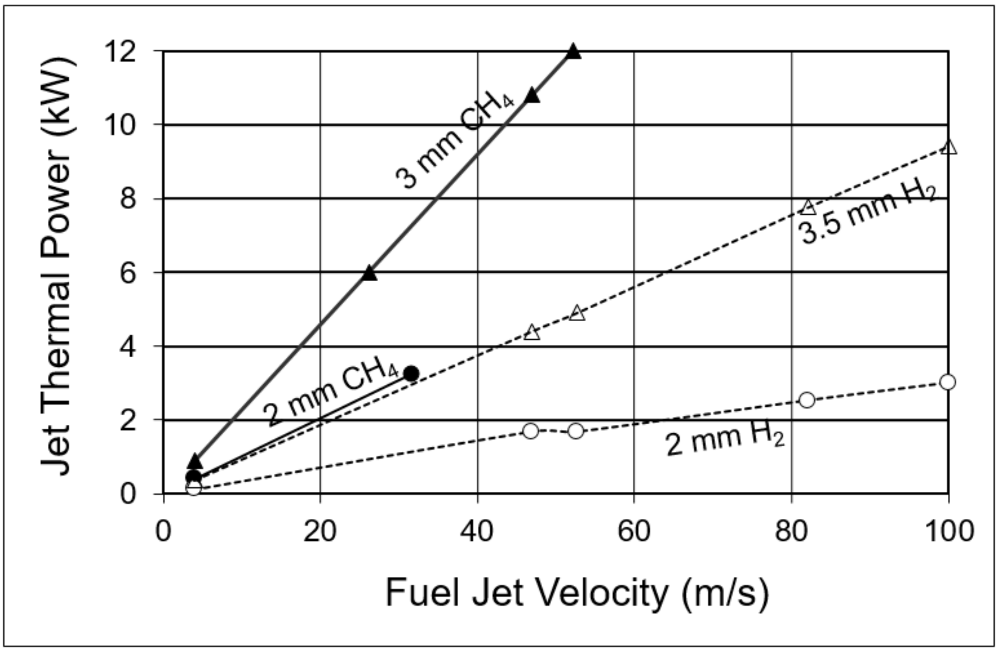

Fig. 2. Thermal power of 2, 3, and 3.5 mm diameter burners at different exit plane fuel jet velocities.

Equation (4) yields jet flame heat release rates, or thermal powers, over a range of fuel jet velocities of H_2 and CH_4. Figure 2 shows the results of such computations with different pipe internal diameters. For the same pipe diameter of 2 mm, CH_4 generates more power than H_2. On the other hand, the CH_4 jets eventually terminate earlier due to blow-off, to which the H_2 jets are more resistant. It also can be seen that a pipe diameter of 3.5 mm, for an H_2 jet is able to generate almost the same power as a CH_4 jet with a pipe diameter of 2 mm, and extending over a greater range of fuel jet velocities.

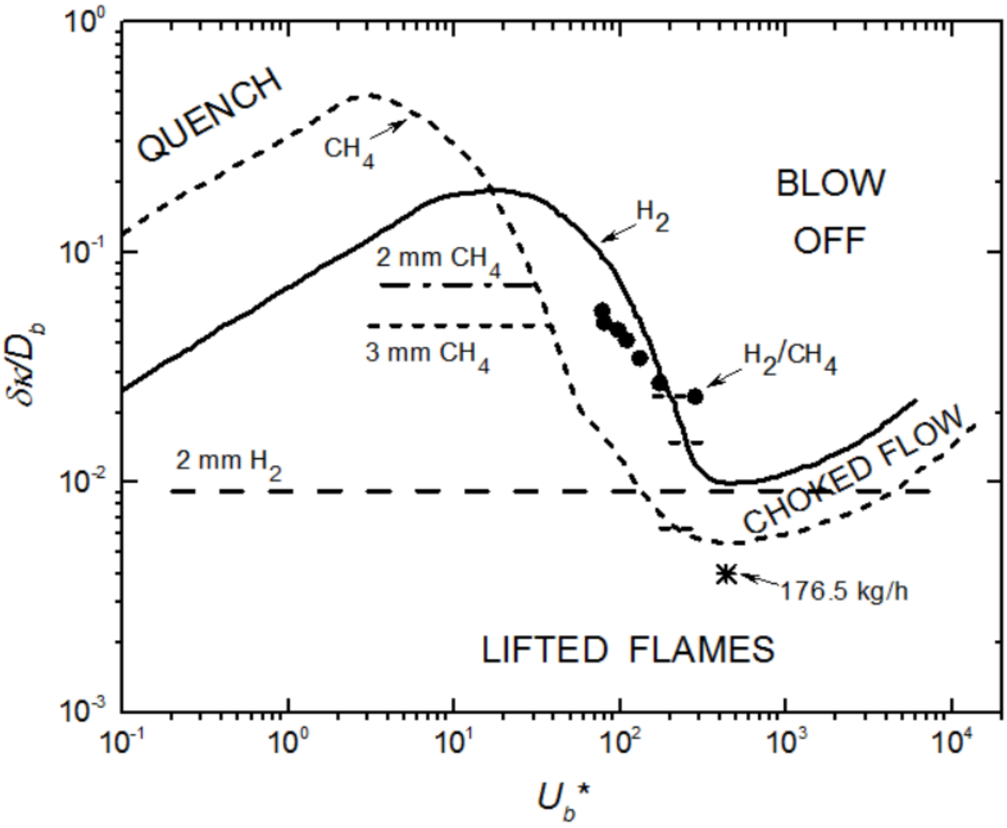

Fig. 3. δ_k/D_b plotted against U_b*. The two CH_4 lines terminate on the CH_4 blow-off curve. Upper four black circle H_2/CH_4, symbols have $H_f = 0.3$, lower three $H_f = 0.5$.

The two 2 mm, and 3 mm diameter, fuel jet pipe relationships in Fig. 2 are transposed to create the more fundamental relationship of δ_k/D_b against U_b* shown in Fig. 3. Although the three broken horizontal lines progress towards blow-off, unlike the CH_4 flames, the H_2 flame does not terminate in blow-off. Figure 3 indicates how its significantly smaller flame thickness and consequent low value of δ_k/D_b have marginally eliminated blow-off, and replaced it with the high reactivity of near-choked and choked flow, which is not part of the present study.

The relevant parametric values just prior to possible blow-off, inevitably lack precision, but are given in Table 1. Basically they are set by δ_k/D and the blow-off curve values of U_b*. They include fuel flow Mach numbers, and jet flame total heat release rates. For CH_4 the smaller value of D of 2 mm has a smaller blow-off velocity of 31.7 m/s, with $U_b* = 30.0$. This compares with a larger blow-off velocity for D = 3 mm of 47 m/s, with U_b^* = 38.0. The reduction in δ_k/D also increases Q from 3.25 to 10.82 kW. With regard to H_2, the low value of D = 2 mm, combines with a fuel flow velocity equal to the sonic velocity of 1,202, to give U^* = 117, and a high heat release rate of 44.7 kW.

Table 1. Operational Details of Blow-off of Jet Flames from Fig. 3.

D, Fuel	δ_k/D	U_b^*	M	u_j (m/s)	ρ_j (kg/m^3)	P_i/P_a	Q (kW)
2 mm, H_2	0.009	(117 Choked Flow)	1.00	1,202	0.099	1.9	44.7
2 mm, CH_4	0.072	30.0	0.007	31.7	0.652	1.0	3.3
3 mm, CH_4	0.048	38.0	0.104	47.0	0.652	1.0	10.8

The large differences in the thermal powers generated by H_2 and CH_4 arise from the contrasting values of two properties: fuel energy density, and convective flow velocity. The ratio of specific H_2 to CH_4 energy density is $M_h \Delta H_\mathrm{h}/M_c \Delta H_\mathrm{c}$, from Eq. (4). With the associated numerical values, this becomes 0.363. The ratio of their flow velocities is that of the appropriate u_j values in Table 1, namely 37.9. Overall, the product of the two ratios gives an overall heat release rate ratio of 13.8, in favour of H_2. However, only the H_2 velocity is sonic. If the comparison had been with a sonic velocity of CH_4, of 424 m/s, the convective flow ratio would be reduced to 2.8, and the of H_2/CH_4 heat release ratio to 1.01.

In contrast, for most practical burners, such as those characterised in Fig. 2, the lower energy densities of H_2 gives CH_4 the higher heat release rates. For the same H_2 and CH_4 fuel jet velocities, and pipe diameters of 2 mm, in Fig. 2 the H_2/CH_4 thermal power ratios are 0.363.

4. Higher Heat Release Rates

The Lifted Flame regime, below the 2 mm H_2 horizontal line in Fig. 3, is one that can support a range of more highly powered flames, at the higher values of U^*, and the lower values of

δ_k/D. It is the regime of the larger sized burners, associated with the flaring of flammable gases [18]. An example of which is the high flow rate, asterisked operational point, marked 176.5 kg/h in Fig. 3. This occurs in a design proposal, for large scale emergency flaring of H_2, from a nuclear reactor, on a 10 mm diameter pipe [19]. The proposed, P_i/P_a is 10, the flame power 5.9 MW, and the flame height, estimated from data generated in [8] to be 8 m. Overall, the regimes in Fig. 3 extend from the quenching of small laminar flames, at the highest values of δ_k/D, to such large scale flaring at the lowest values. High velocity flaring makes extinction by cross flows less likely. Although not considered in the present study, it is featured in [19].

It has been shown how compensation for the low specific energy of H_2 can be achieved through its high blow-off velocity, coupled with its high sonic velocity. Table 1 shows the relatively low subsonic blow-off conditions for the blow-off of two CH_4 jet flames from small pipe burners of 2 and 3 mm diameter. Higher blow-off velocities and heat release rates become possible on larger diameter burners. In this context, it is a useful guide to indicate on blow-off curves the conditions for the onset of a sonic velocity.

The onset of this regime, through a sufficiently high pipe diameter and the sonic velocity at, or near, blow-off, was identified for both fuels, through trial calculations. These involved variations in values of M, δ_k/D, and U_b*. The following values emerged as being close to this sonic onset: for CH_4, u_j = 424 m/s, D = 26 mm, with δ_k/D = 0.006, and U_b* = 266, giving a total heat release rate of 7.26 MW. In practice, the transition does not occur at a precise point, but probably somewhere along the short horizontal line, shown cutting the broken CH_4 blow-off curve in Fig. 3.

For H_2, such transition conditions are u_j = 1,202 m/s, D = 1.2 mm with δ_k/D = 0.015, and U_b* = 143, with a relatively small total heat release rate of 16.1 kW, arising from the small pipe diameter. Again, transition might occur along the short horizontal line shown cutting the continuous H_2 blow-off boundary curve in Fig. 3. A dominating factor is that, for a given fuel jet velocity, a minimum pipe diameter is necessary to sustain a flame. In the present study the limiting diameters predicted for the onset of stable flames were close to those measured for H_2, in [20], and for CH_4, in [21].

5. Blended Fuel Characteristics

Figure 2 indicates the loss that would occur in jet thermal power, were the same flow velocities to be maintained, but with CH_4 substituted for H_2. The loss is a consequence of the greater mass specific energy of CH_4. It could be countered by a larger flow velocity for H_2, than that employed for CH_4. The power loss might also be countered, as shown in Fig. 2, by a larger flow rate through a larger diameter pipe. Another approach might be to reduce the energy deficit by substituting only a fraction of the CH_4, by H_2 and burning a CH_4/H_2 blend, with a consequently smaller increase in u_j than with a complete conversion. The use of such a blended fuel requires knowledge of the energy contribution from each fuel at the different flow velocities.

Total heat release rates, as well as the separate contributions, were calculated, as a function of fuel jet velocity, in a pipe of 2 mm diameter. This was done for increasing partial substitution of CH_4 by H_2, with the results shown in Fig. 4, for $H_f = 0.2$, 0.3, 0.5 and 0.8. The total power generated, shown by the full line, decreases as the proportion generated by H_2 increases. Some blow-off limits for these different CH_4/H_2 blends are indicated by the black circles in Figs. 1 and 3. As shown in Table 1, the blow-off velocities for a 2 mm diameter-pipe are 31.7 and 1,202 m/s for CH_4 and H_2, respectively, with heat release rates of 3.3 and 44.7 kW. Figure 4 in [10] shows the sharp increase in blow-off velocity that occurs with increase in H_2 concentration.

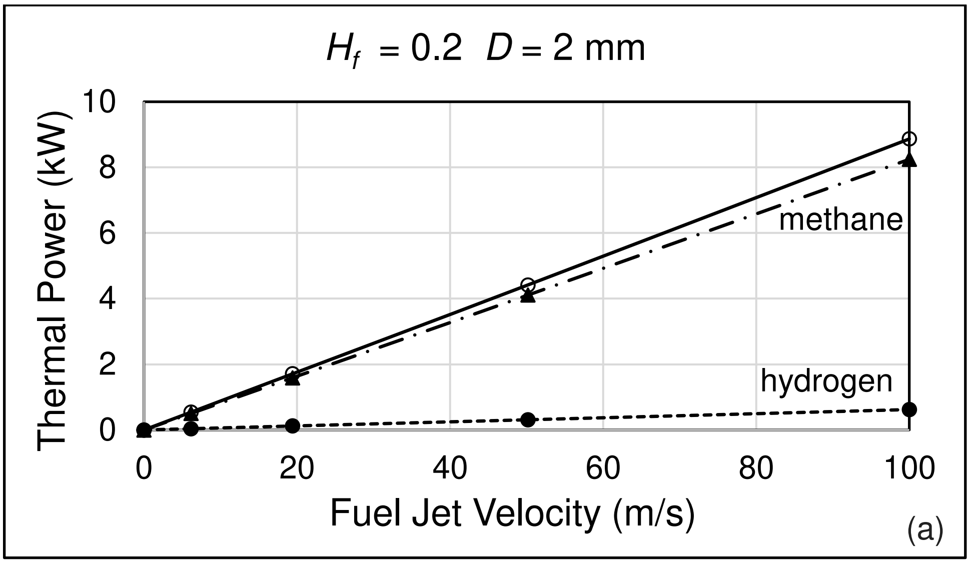

H_f = 0.2 D = 2 mm
Thermal Power (kW)
Fuel Jet Velocity (m/s)
methane
hydrogen
(a)

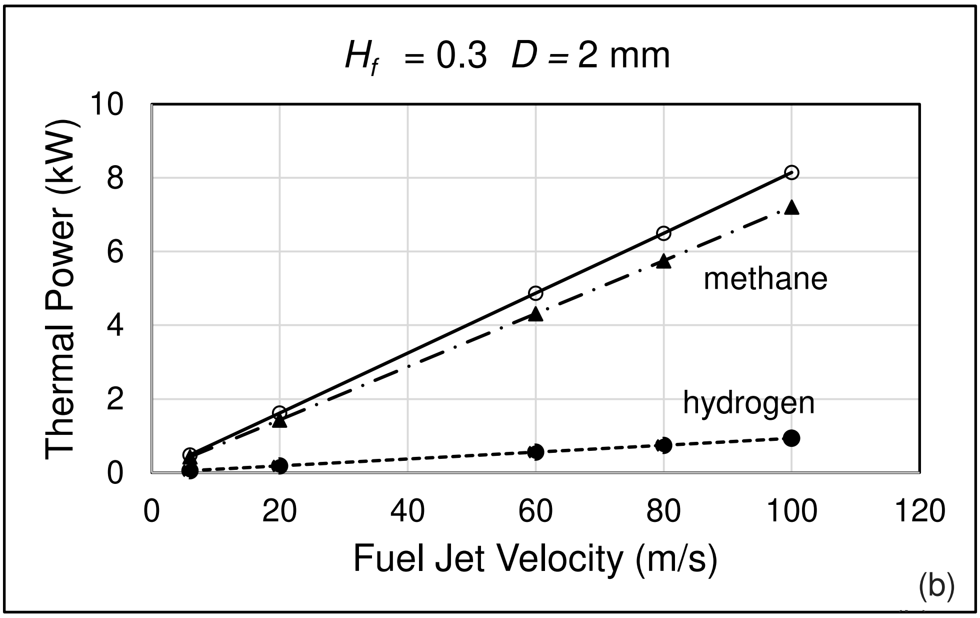

H_f = 0.3 D = 2 mm
Thermal Power (kW)
Fuel Jet Velocity (m/s)
methane
hydrogen
(b)

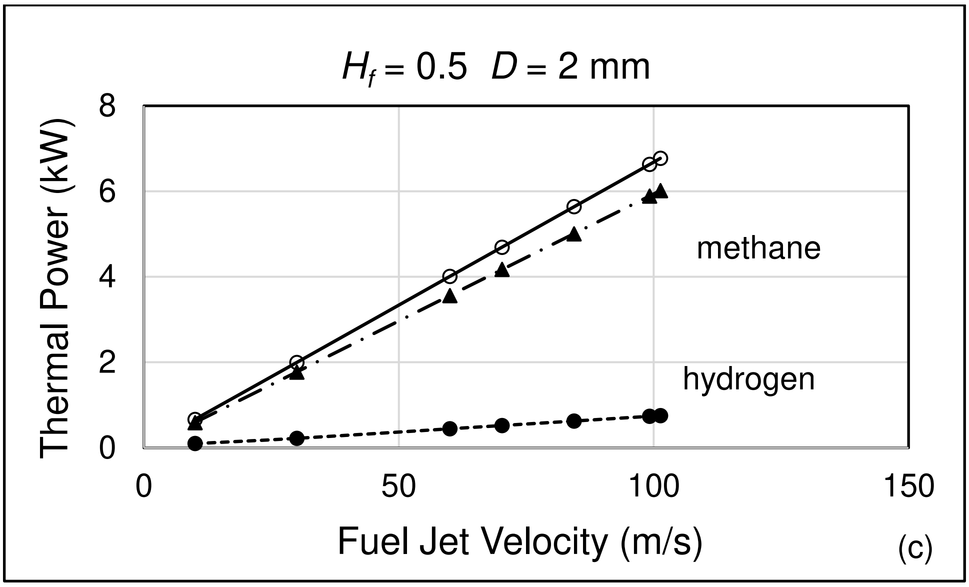

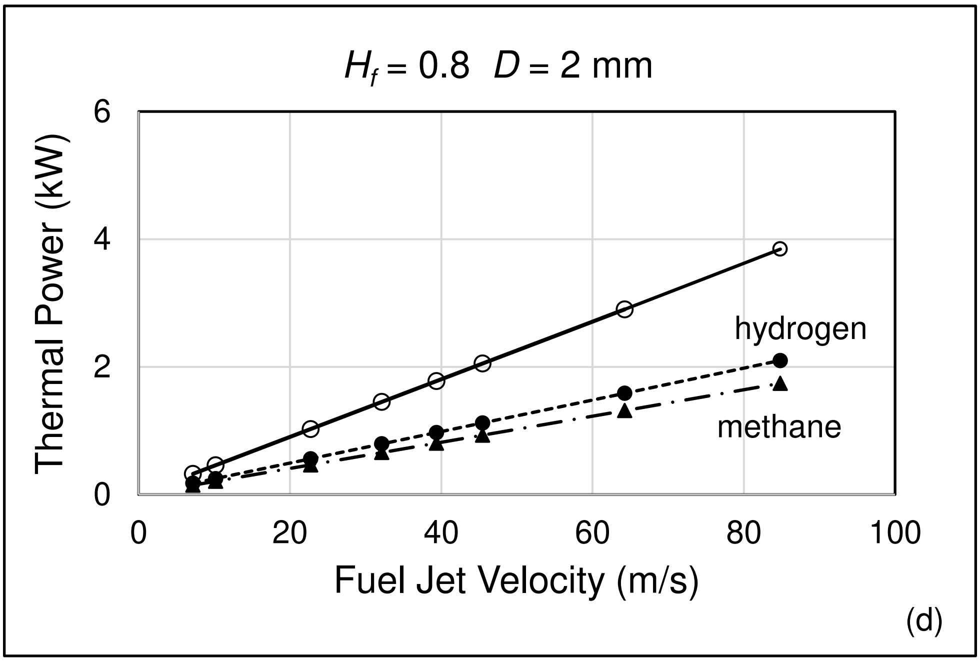

Fig. 4. Effect of increasing H_f from 0.2 to 0.8 on fuel jet power, D = 2 mm.

Figures 4 (a) to (d) show the effects of progressively increasing the proportion of H_2 in the mixture. Solid lines indicate the total heat release rate of the mixture, dashed lines give the contributions of each component.

As with the unblended fuels, the thermal power of a jet flame increases linearly with u_j. The overall trend is a decline in thermal power with increasing H_f. The lower mass specific energy density of H_2 inevitably reduces the thermal power, and only when H_f has reached 0.8 does the H_2 contribution to the overall heat release rate exceed that of CH_4. There is some compensation for this loss, in that the decrease in the value of δ_k/D makes it possible to attain higher values of U^* before blow-off.

6. Strategies for Conversion from Natural Gas to Hydrogen

Jet flame performances of all the different blends are now considered for two modes of operation, for values of H_f between 0 and 1.0. The first mode retains a constant blend jet velocity of 50 m/s, and derives the consequent heat release rates for the different blends. The second retains a heat release rate of 0.5 kW, and derives the jet velocities necessary to maintain this. In both modes, the pipe diameter is 2 mm.

Figure 5 shows the first mode, with an accompanying heat release rate that decreases linearly with H_f over the full range. The figure also demonstrates how the mass fraction of H_2 in the blend must increase sharply, as H_f approaches unity. About half the mass of H_2 burns at half the original heat release rate.

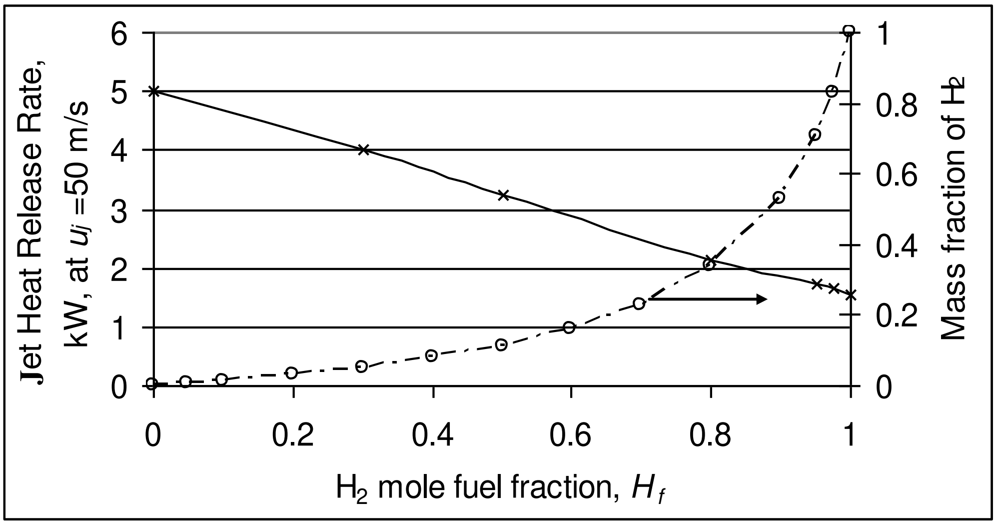

Fig. 5. Variation of blend jet heat release rate, with mole and mass fractions of H_2, for a jet velocity of 50 m/s and pipe diameter of 2 mm.

Figure 6 shows the second mode with the increasing jet velocity of the blend to maintain a constant heat release rate of 0.5 kW, increasing more sharply with H_f. The complete conversion from CH_4 to H_2 necessitates an increase in jet velocity from 4.9 to 16.2 m/s, a ratio of 3.3, to maintain 0.5 kW.

The heat release rate of 0.5 kW in this figure is more typical of a jet flame within an array of flames on a hob burner, and a stagnation to atmospheric pressure ratio, P_i/P_a, of about 1.02 or 1.03. There are limited data on the associated small, low velocity, jet flame lift-off distances [22]. Peters [23] suggested a lift-off distance of 4 pipe diameters, at a velocity of 16 m/s.

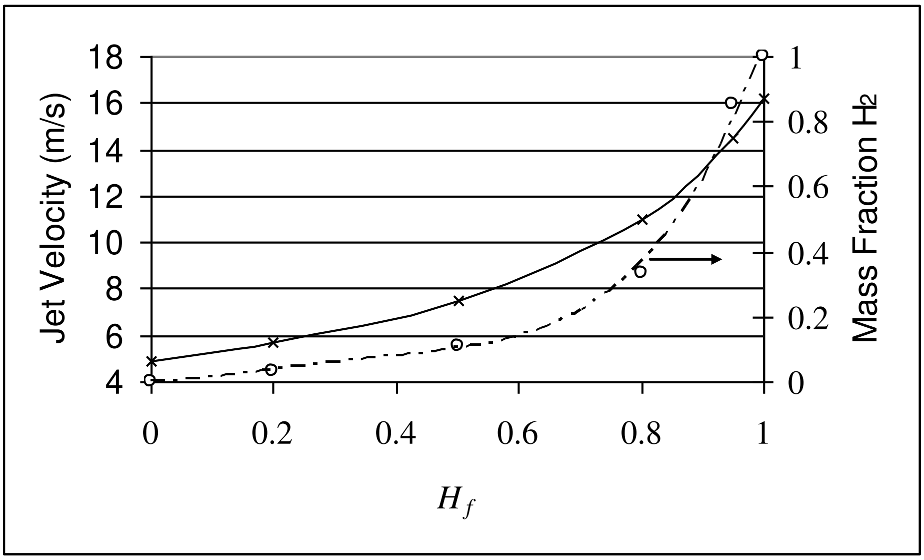

Fig. 6. Variation in blend jet velocity necessary to maintain a heat release rate of 0.5 kW, at different values of H_f, with a pipe diameter of 2 mm.

Amelioration of the problems of inadequate heat release rate with H_2 might be sought through a combination of increases in both velocity and burner diameter. A small increase in diameter, with some increase in u_j might be an effective compromise. An increase in pipe diameter might be preferred to three fold increases in jet velocity.

Another approach is only partially to substitute H_2 for CH_4. With the high sensitivity of the necessary jet velocity to the higher values of H_f, it is difficult to see any advantage in a mixture with small proportions of CH_4. However, a noteworthy aspect of Fig. 6 is the relatively small change in the necessary jet velocity to maintain a fairly steady heat release rate at the lower values of H_f, of up to about 0.2. In this regime, an H_2/CH_4 flame is closest to a CH_4 flame in its characteristics. However, this is a rather marginal benefit, bearing in mind, from Fig. 4 (a), the very small contribution of H_2 to the overall energy, and that decarbonisation is the main motivation for the conversion.

Interestingly, Heats of Reaction and the overall reactions show a reduction in O_2 consumption of about 20%, when H_2 replaces CH_4, for a given heat release rate.

7. Conclusions

1. Previous fundamental computational and experimental studies of jet flames have facilitated this present investigation, predominantly involving small burner jet flames of CH_4 and H_2, both separately, and blended. The motivation has been to apply this understanding to the conversion of burners from natural gas to hydrogen.

2. H_2 has the disadvantage of a low mass specific energy, about 0.35 that of CH_4. This reduces the heat release rate at CH_4 fuel jet velocities.

3. H_2 has many advantages as a fuel: a high burning velocity, small flame thickness, and resistance to flame quenching. Its potential for operation at the lower values of δ_k/D enables higher jet velocities to be attained, before blow-off occurs. Combined with its high acoustic velocity, this enables high subsonic heat release rates to be obtained. These can be an order of magnitude higher those in small power, natural gas, burners.

4. The possibility of high subsonic Mach numbers combined with high acoustic and burning velocities, enable high jet flame heat release rates to be achieved.

5. In contrast, to retain the same heat release rates in burners as with CH_4, H_2 would require an approximately three fold increase in jet velocity, with an unchanged pipe diameter.

6. Alternatively, an increase in pipe diameter from 2 mm (CH_4) to 3.5 mm (H_2), with no change in fuel jet velocity, would almost maintain the same jet heat release rate.

7. Partial substitution of H_2 for CH_4 is possible. But only when H_f has reached a value of 0.8 does the H_2 contribution to the overall heat release rate exceed that of CH_4. With values of H_f in the region of 0.2, the burning characteristics of H_2/CH_4 flames are at their closest to those of

CH_4 flames, and minimal change would be required for such a conversion. This yields only a limited operational benefit, as the H_2 would only contribute about 7% to the overall flame power.

8. The attainment of the acoustic velocity, at the indicated point on a blow-off curve by the fuel, just prior to blow-off, generates the highest heat release rate short of supersonic flow.

Acknowledgements

A.P. gratefully acknowledges the financial support of the Royal Society in the form of a Newton International Fellow Alumnus.

References

[1] Thurnheer T, Soltic P, Dimopoulos Eggenschwiler P. S.I. engine fuelled with gasoline, methane and methane/hydrogen blends: Heat release and loss analysis. Int. Jour. Hydrogen Energy. 2009;34(5):2494–2503. https://doi.org/10.1016/j.ijhydene.2008.12.048

[2] Karim GA, Wierzba I, Al-Alousi Y. Methane-hydrogen mixtures as fuels. Int. Jour. Hydrogen Energy. 1996:21(7): 645–31.https://doi.org/10.1016/0360-3199(95)00134-4

[3] Fairweather M, Ormsby MP, Sheppard CGW, Woolley R. Turbulent burning rates of methane and methane-hydrogen mixtures. Combust. Flame. 2009;156(4):780–90. http://dx.doi.org/10.1016/j.combustflame.2009.02.001

[4] Büyükakın MK, Öztuna S. Numerical investigation on hydrogen-enriched methane combustion in a domestic back-pressure boiler and non-premixed burner system from flame structure and pollutants aspect. Int. Jour. Hydrogen Energy. 2020 https://doi.org/10.1016/j.ijhydene.2020.03.117

[5] Bradley D, Gaskell PH, Gu XJ. The mathematical modelling of lift-off and blow-off of turbulent non-premixed methane jet flames at high strain rates. Proc. Combust. Inst. 1998;27:1199–1206. https://doi.org/10.1016/S0082-0784(98)80523-7

[6] Bradley D, Gaskell PH, Gu XJ. The modelling of aerodynamic strain rate and flame curvature effects in premixed turbulent combustion. Proc. Combust. Inst. 1998;27:849–56. https://doi.org/10.1016/S0082-0784(98)80481-5

[7] Bradley D, Emerson DR, Gaskell PH, Gu XJ. Mathematical modelling of turbulent non-premixed piloted-jet flames with local extinctions. Proc. Combust. Inst. 2002;29:2155–62. https://doi.org/10.1016/S1540-7489(02)80262-0

[8] Bradley D, Gaskell PH, Gu XJ, Palacios A. Jet flame heights, lift-off distances, and mean flame surface density for extensive ranges of fuels and flow rates. Combust. Flame. 2016;164:400–9. http://dx.doi.org/10.1016/j.combustflame.2015.09.009

[9] Göttgens J, Mauss F, Peters N. Analytic approximations of burning velocities and flame thicknesses of lean hydrogen, methane, ethylene, ethane, acetylene and propane flames. Proc. Combust. Inst. 1992;24:129–35. https://doi.org/10.1016/S0082-0784(06)80020-2

[10] Wu Y, Lu Y, Al-Rahbi IS, Kalghatgi GT. Prediction of the lift off, blowout and blow off stability limits of pure hydrogen and hydrogen/hydrocarbon mixture jet flames. Int. Jour. of Hydrogen Energy. 2009; 34:5940–5. https://doi.org/10.1016/j.ijhydene.2009.01.084

[11] Hu Erjiang, He Jiajia, Jin Chun, Zheng Jianjun. Experimental and numerical study on laminar burning characteristics of premixed methane-hydrogen-air flames. Int. J. Hydrogen Energy. 2009; 34:4876–88. https://doi.org/10.1016/j.ijhydene.2009.03.058

[12] Palacios A, Bradley D. Generalised correlations of blow-off and flame quenching for sub-sonic and choked jet flames. Combust. Flame. 2017;185:309–18. https://doi.org/10.1016/j.combustflame.2017.07.019

[13] Massey BS. Mechanics of fluids. 6th ed. US: Van Nostrand Reinhold (International); 1989.

[14] Houghton EL, Brock AE. Tables for the compressible flow of dry air. London: Edward R Arnold (Publishers); 1961.

[15] Morley C. GasEq: a chemical equilibrium program for windows, http://www.gaseq.co.uk/; 2005 [accessed 11 August 2020].

[16] Ewan BC, Moodie K. Structure and velocity measurements in underexpanded jets. Combust. Sci. Tech. 1986;45:275–88. https://doi.org/10.1080/00102208608923857

[17] Hu Longhua, Wang Qiang, Delichatsios M, Lu Shouxiang, Tang Fei. Flame radiation fraction behaviors of sooty buoyant turbulent jet diffusion flames in reduced and normal atmospheric pressures and a global correlation with Reynolds number. Fuel. 2014;116:781–6. https://doi.org/10.1016/j.fuel.2013.08.059

[18] Palacios A, Bradley D, Wang Qiang, Li Xin, Hu Longhua. Air/fuel mixing in jet flames. Proc. Combust Inst. 2020;38. In press. https://doi.org/10.1016/j.proci.2020.07.083

[19] Palacios A, Bradley D. Hydrogen generation, and its venting from nuclear reactors. Fire Saf. J. 2020;113:102968. https://doi.org/10.1016/j.firesaf.2020.102968

[20] Kalghatgi GT. Blow-out stability of gaseous jet diffusion flames. Part 1: in still air. Combust. Sci. Tech. 1981;26:233–9. https://doi.org/10.1080/00102208108946964

[21] McCaffrey BJ, Evans DD. Very large methane jet diffusion flames. Proc. Combust. Inst. 1986;21:25–31.

[22] Bradley D, Casal J, Palacios A. Prediction of lift-off distance in choked and subsonic hydrogen jet fires. Catal. Today. 2019;329:221–4. https://doi.org/10.1016/j.cattod.2017.11.024

[23] Peters N. Turbulent combustion. UK: Cambridge University Press; 2000.